J|A|C|S
ARTICLES
Published on Web 01/15/2004

An Investigation of the Mechanisms of Electronic Sensing of Protein Adsorption on Carbon Nanotube Devices

Robert J. Chen,[†,§] Hee Cheul Choi,[†,§,||] Sarunya Bangsaruntip,[†] Erhan Yenilmez,[†] Xiaowu Tang,[†] Qian Wang,[†] Ying-Lan Chang,[‡] and Hongjie Dai*[,†]

Contribution from the Department of Chemistry, Stanford University, Stanford, California 94305, and Agilent Laboratories, Agilent Technologies, Inc., 3500 Deer Creek Road, Palo Alto, California 94304

Received September 24, 2003; E-mail: hdai@stanford.edu

Abstract: It has been reported that protein adsorption on single-walled carbon nanotube field effect transistors (FETs) leads to appreciable changes in the electrical conductance of the devices, a phenomenon that can be exploited for label-free detection of biomolecules with a high potential for miniaturization. This work presents an elucidation of the electronic biosensing mechanisms with a newly developed microarray of nanotube "micromat" sensors. Chemical functionalization schemes are devised to block selected components of the devices from protein adsorption, self-assembled monolayers (SAMs) of methoxy(poly-(ethylene glycol))thiol (mPEG-SH) on the metal electrodes (Au, Pd) and PEG-containing surfactants on the nanotubes. Extensive characterization reveals that electronic effects occurring at the metal−nanotube contacts due to protein adsorption constitute a more significant contribution to the electronic biosensing signal than adsorption solely along the exposed lengths of the nanotubes.

Introduction

Carbon nanotubes are a novel class of nanomaterials that demonstrate remarkable versatility and wide applicability, from serving as a model system for elucidating transport phenomena in 1D[1,2] to being woven into polymeric nanocomposites for superfrabrics.[3] In addition, the significant conductance change of single-walled carbon nanotubes (SWNTs) in response to the physisorption of ammonia and nitrogen dioxide demonstrates their ability to act as extremely sensitive gas-phase chemosensors.[4−8] Such sensitivity has been recently demonstrated to be transferable to the aqueous phase for small biomolecule and protein detection in physiological solutions.[9−11] That is, binding of proteins to the surface of carbon nanotube devices or to a suitable binding receptor immobilized on the devices results in a conductance change as well. By judicious immobilization of first layer protein, it is then a simple matter of monitoring for a conductance change of the nanotube biosensor in order to detect a second layer binding event, thus obviating the need for prelabeling techniques such as those required in fluorescence-based methods.

However, several fundamental and technological challenges remain to be addressed before nanotube biosensors can be fully exploited for real-life applications such as in medical diagnostics, proteomics arrays, and gene chips. The next generation of nanotube biosensors will require highly miniaturized, arrayable designs that can be functionalized and monitored in multiplex fashion. Further, a clear understanding of how electrical conductance is affected by protein adsorption is currently lacking but essential to continuing efforts to optimize nanotube biosensor designs. One proposal for the mechanism is that charges on the surface of proteins exert gating effects or charge transfer to nanotubes, thereby causing changes in the electrical conductance of the nanotube FETs.[9,11] This is essentially what has been suggested for nanowire-based biosensors.[12] A second possibility is that protein adsorption on the devices affects the dielectric constant of the electrical double layer in aqueous solution, thereby changing the gate efficiency of the electrolyte.[9,13] In our recent nanotube biosensor demonstration, it is pointed out that charge alone does not account for the sensing mechanism and that a more systematic investigation is required. Here, we present a new design for SWNT-based biosensors to address these issues. With a large number of high quality devices mass-

[†] Stanford University.
[‡] Agilent Technologies, Inc..
[§] These author contributed equally.
[||] Current address: Department of Chemistry, Pohang University of Science and Technology (POSTECH) San 31, Pohang, Korea 790-874.

(1) Dai, H. *Surf. Sci.* **2002**, *500*, 218.
(2) McEuen, P. L.; Fuhrer, M. S.; Park, H. K. *IEEE Trans. Nanotechnology* **2003**, *1*, 78.
(3) Shaffer, M. S. P.; Windle, A. H. *Adv. Mater*. **1999**, *11*, 937.
(4) Qi, P.; Vermesh, O.; Grecu, M.; Javey, A.; Wang, O.; Dai, H.; Peng, S.; Cho, K. J. *Nano Lett.* **2003**, *3*, 347.
(5) Kong, J.; Franklin, N. R.; Zhou, C. W.; Chapline, M. G.; Peng, S.; Cho, K. J.; Dai, H. *Science* **2000**, *287*, 622.
(6) Valentini, L.; Armentano, I.; Kenny, J. M.; Cantalini, C.; Lozzi, L.; Santucci, S. *Appl. Phys. Lett.* **2003**, *82*, 961.
(7) Li, J.; Lu, Y. J.; Ye, Q.; Cinke, M.; Han, J.; Meyyappan, M. *Nano Lett.* **2003**, *3*, 929.
(8) Goldoni, A.; Larciprete, R.; Petaccia, L.; Lizzit, S. *J. Am. Chem. Soc*. **2003**, *125*, 11329.
(9) Chen, R. J.; Bangsaruntip, S.; Drouvalakis, K. A.; Wong Shi Kam, N.; Shim, M.; Li, Y. M.; Kim, W.; Utz, P. J.; Dai, H. *Proc. Natl. Acad. Sci. U.S.A.* **2003**, *100*, 4984.
(10) Besteman, K.; Lee, J.-O.; Wiertz, F. G. M.; Heering, H. A.; Dekker, C. *Nano Lett.* **2003**, *3*, 727.
(11) Star, A.; Gabriel, J.-C. P.; Bradley, K.; Gruner, G. *Nano Lett.* **2003**, *3*, 459.
(12) Cui, Y.; Wei, Q. Q.; Park, H. K.; Lieber, C. M. *Science* **2001**, *293*, 1289.
(13) Bard, A. J.; Faulkner, L. R. *Electrochemical Methods; Fundamentals and Applications*; John Wiley & Sons: New York, 1980; Chapter 1.

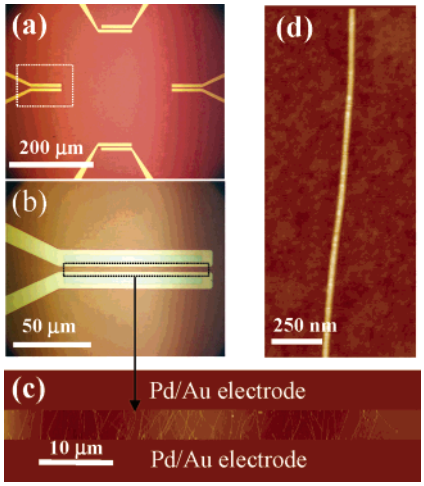

Figure 1. Optical and atomic force microscopy (AFM) images of a four-device array of SWNT micromat sensors (type I device without any chemical functionalization). (a) An optical microscopy image showing an array of four micromat devices on a chip. (b) A close-up optical image of one device. (c) An AFM image of the gap region between two metal contact electrodes in a micromat device. A typical device comprises roughly ~100 carbon nanotubes with diameters in the range of 1−3 nm. A gap of 5 μm between the electrodes ensures each nanotube bridges completely, thus approaching a parallel network. (d) A close-up AFM image of a clean individual nanotube (diameter = 2.8 nm) in the device.

produced by microfabrication techniques, we carry out a detailed investigation into the mechanisms by which biomolecules in solution are able to bring about a conductance change through adsorption on the surfaces of the devices.

The nanotube sensor design used here consists of an array of four micromat sensors on SiO_2/Si chips. Each micromat sensor comprises multiple SWNTs connected roughly in parallel across two closely spaced (5 μm) bridging metal electrodes (Pd or Pd/Au, Figure 1). Three types of devices with different surface functional groups are prepared (Scheme 1) for the systematic investigation of the biosensing mechanism: (1) unmodified as-made devices (device type I); (2) devices with mPEG-SH SAMs formed on, and only on, the metal contact electrodes (device type II); and (3) devices with mPEG-SH SAMs on the metal contacts and a Tween 20 coating on the carbon nanotubes (device type III). With these three types of devices, first layer nonspecific binding and selective second layer detection of various proteins are studied with atomic force microscopy (AFM), quartz crystal microbalance (QCM), X-ray photoelectron spectroscopy (XPS), and electrical measurements.

Methods

Materials. Human serum albumin (HSA), bovine serum albumin (BSA), and avidin were purchased from Sigma-Aldrich. Human chorionic gonadotropin (hCG), its monoclonal antibody α-hCG, and polyclonal human IgG (hIgG) were purchased from BiosPacific (Emeryville, CA). Methoxy(poly(ethylene glycol))thiol (mPEG-SH, MW 5000) was obtained from Nektar Therapeutics. Other chemicals were purchased from Sigma-Aldrich. All proteins and chemicals were used without further purification.

X-ray Photoelectron Spectroscopy (XPS). XPS measurements were carried out on a PHI Quantum 2000 scanning microprobe equipped with an angle-resolved hemispherical electron energy analyzer and a base system pressure of 1×10^{-9} Torr. All measurements were performed using the Al Kα line with a photon-energy of 1486.6 eV. Charge compensation during acquisition was applied using the improved dual neutralization capability including an electron flood gun and an ion gun. For the XPS study, SiO_2 substrates metallized via thermal evaporation with Pd (30 nm thick) or Pd/Au (15 nm/15 nm) were used.

Scheme 1. Schematic Flowchart of Microfabrication Processes for the Preparation of Devices[a]

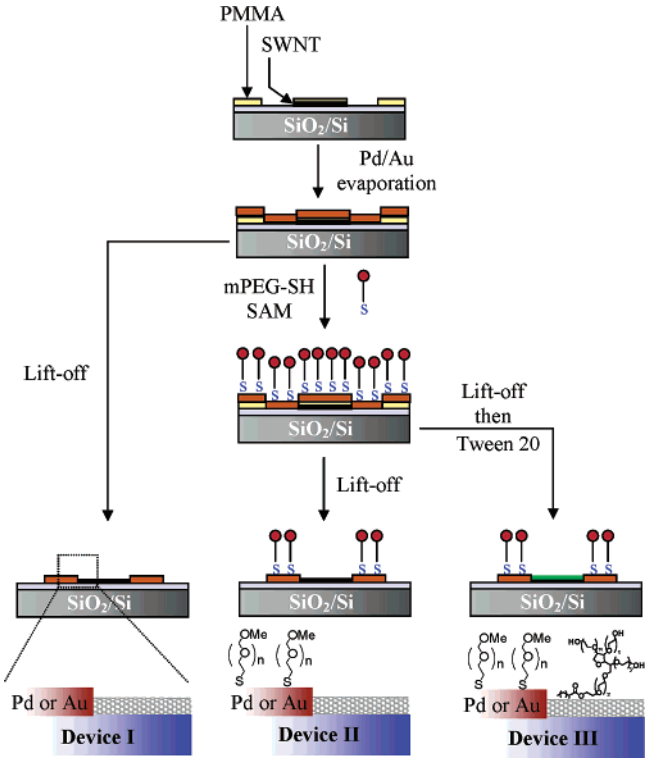

[a] A regular device comprised of metal contact with multiple SWNT connections is prepared by lift-off the photoresist layer immediately after metal evaporation (device type I). Formation of mPEG-SH SAM followed by lift-off affords device type II. Further treatment of type II devices with a Tween 20 solution leads to device type III.

Quartz Crystal Microbalance Experiments. QCM measurements were performed with a Q-Sense D-300 instrument (Q-Sense Inc, Newport Beach, CA) on optically polished quartz crystal substrates (5 MHz, AT cut) coated with Au. Frequency shifts due to mass uptake were measured at the third harmonic resonance of the crystal. For protein adsorption studies on Pd, quartz crystal substrates were further metallized with palladium via thermal evaporation to a thickness of 30 nm (with a 5 nm titanium adhering layer). mPEG-SH-coated Au and Pd substrates were produced by immersing the metal-coated quartz crystals in an aqueous solution of mPEG-SH (5 mM) overnight, followed by thorough rinsing with deionized water (R = 18 MΩ).

Nanotube Micromat Sensor Arrays. Micromat devices were produced at the 4 in. wafer scale via patterned SWNT growth[4,14,15] followed by standard microfabrication techniques on SiO_2/Si wafers (thermal oxide thickness ≈ 500 nm). SWNTs were first synthesized by chemical vapor deposition of methane on iron nanoparticles[15] on top of which Pd electrodes spaced at 5 μm were formed by evaporation and lift-off techniques as shown in Scheme 1. The diameters of the SWNTs synthesized by this method are in the range of 1−4 nm with a mean of ~2 nm. For Au-covered metal contacts, Pd was evaporated first to a thickness of 15 nm, followed by 15 nm of Au prior to lift-off of photoresist. Note that throughout this work, both Pd- and Pd/Au-contacted devices were found to exhibit similar electronic characteristics and biosensing behavior. Optical images of these devices are shown in Figure 1a and b. AFM images show that the final micromat device consists of multiple (~100) SWNTs bridging the electrode gap in a quasi-parallel fashion (Figure 1c) and that the surface of a typical

(14) Kong, J.; Soh, H. T.; Cassell, A. M.; Quate, C. F.; Dai, H. *Nature* **1998**, *395*, 878.
(15) Yenilmez, E.; Dai, H. Unpublished result.

Table 1. Summary of Whether Type I, II, and III Devices Exhibit Electrical Conductance Changes upon Exposure to Various Proteins in Solutions

proteins/ devices	device I (Pd/Au)	device II (mPEG-SH on Pd/Au)	device III (mPEG-SH on Pd/Au and Tween 20 on nanotubes)
BSA	yes	no	n/a
HSA	yes	no	n/a
hCG	yes	no	n/a
α-hCG	yes	no	n/a
hIgG	yes	no	n/a
avidin	yes	yes	no

nanotube is clean after the microfabrication processing steps (Figure 1d). The final chip (1 cm × 1 cm) comprises four of these devices, each with independent electrodes, lying in a diameter of <1 mm, such that a homemade static liquid cell can be used to immerse all four devices in solution. Typical electrical measurements were performed with a semiconductor parameter analyzer capable of monitoring all four devices simultaneously during protein adsorption.

Devices prepared in this way (device type I, Scheme 1), without any chemical functionalization, were used to investigate protein adsorption on both carbon nanotubes and the metal contacts. To study adsorption of proteins on carbon nanotubes alone (and not on the metal contacts), the electrodes were selectively passivated with mPEG-SH SAMs (device type II, Scheme 1). Following Pd (or Pd/Au) evaporation, the devices were exposed to an aqueous solution of mPEG-SH (5 mM) at room temperature overnight, after which they were rinsed thoroughly with deionized water to remove any nonchemisorbed mPEG-SH molecules. Acetone was then used to lift off the poly(methyl methacrylate) (PMMA) photoresist layer that had been protecting the carbon nanotubes from exposure to the mPEG-SH solution. This afforded type II devices in which the metal electrodes were selectively coated with mPEG-SH while the nanotubes remained bare and open to protein adsorption (Figure 1d).

For the prevention of protein adsorption on both carbon nanotubes and metal contacts, i.e., whole device passivation (device type III, Scheme 1), an aqueous solution of the surfactant Tween 20 (0.1% w/w) was introduced to a type II device (as described above) that had been loaded into the static liquid cell. After a 1 h exposure, the solution of Tween 20 was rinsed out thoroughly with deionized water. Earlier results have shown that Tween 20 adsorbs on SWNT surfaces irreversibly without desorption in aqueous solutions and that the PEG groups on Tween 20 render nanotubes protein resistant.[9,16]

Electrical Measurement. For electrical measurements of the devices during exposure to proteins, a micromat chip was loaded into the homemade static liquid cell with the four sensor devices on the chip electrically wired to a semiconductor parameter analyzer (4156C, Agilent). The devices were stabilized in a 10 mM sodium phosphate buffer solution (pH 7), and a platinum wire was inserted as a gate electrode (V_{gs}). When biased at $V_{gs} = 0$ (with respect to V_d), the gate electrode eliminates electrical noise caused by the addition of analyte. Source-drain (SD) bias of 10 mV and $V_{gs} = 0$ were maintained throughout the measurements. For $I-V_{gs}$ measurements before and after protein adsorption, the gate electrode potential was swept from −350 mV to +350 mV with an SD bias of 10 mV.

Results and Discussion

Electrical conductance of the three types of devices upon the addition of various protein molecules was monitored, and the results were summarized in Table 1. While device type I showed significant conductance change with protein adsorption, device type II with an mPEG-SH SAM on the metal electrodes did not give any conductance change except in the case of the protein avidin (Table 1).

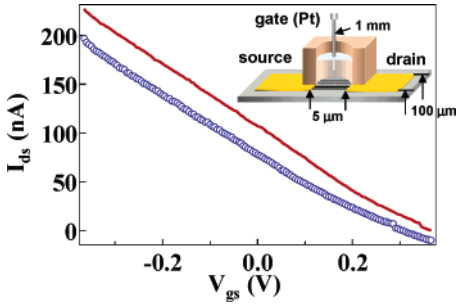

Figure 2. Semiconducting nature of micromat nanotube devices can be probed with current (I_{ds}) vs gate voltage (V_{gs}) measurements (bias = 10 mV) via a platinum wire top gate electrode inserted into the solution (inset). The main panel shows I_{ds} vs V_{gs} before (solid line) and after hCG adsorption (circle) on a type I device. A downward shift in the overall conductance is seen after protein adsorption. It should be noted that a device with an $I-V_{gs}$ curve showing near-depletion (zero SD conductance at +350 mV V_{gs}) was chosen especially for this particular measurement. This near-depletion arises from a larger-than-usual ratio of semiconducting to metallic nanotubes bridging the electrodes, which also results in a lower conductance overall. Typical devices used for all other measurements show higher conductance in general due to a relatively higher proportion of metallic nanotubes.

Nonspecific Binding (NSB). Previous studies on protein adsorption have shown that many different types of proteins adsorb spontaneously onto carbon nanotubes from aqueous solution.[10,16] This adsorption results in a decrease in the electrical conductance of the nanotubes through what is presumed to be charge injection from or a field effect induced by electron-donating (or -withdrawing) groups,[9,11] such as from the lysine residues on the exterior of proteins. Regardless of the mechanism, the modulation of conductance by physisorbed molecules is known to require semiconducting SWNTs to be present in the devices. The current micromat design comprises a considerable fraction of semiconducting nanotubes (~60−70%) and thus exhibits semiconducting characteristics as a whole.[4,17] Figure 2 shows conductance versus top gate voltage plots for a micromat device immersed in an aqueous buffer solution (sodium phosphate, 10 mM) before (solid line) and after exposure to 100 nM hCG (circle). Within a range of −350 to +350 mV of gate voltage, the conductance of the device can be modulated from ~230 nA to near depletion (i.e., zero conductance). As a general rule, this high susceptibility to gate modulation is a good predictor for sensitivity to biomolecular adsorption at the surface.

Sensitivity to protein adsorption is indeed observed for type I devices in which both nanotubes and their metal contacts are exposed to solution; a significant conductance change is seen in such devices upon protein adsorption (Figures 2 and 3). Type II devices, however, in which the metal contacts are protected from NSB by mPEG-SH, behave significantly differently. This offers considerable insight into the mechanism by which protein adsorption is able to modulate the conductance of SWNT-FETs, as is further discussed below.

Device Type I. Real-time detection of protein adsorption can be observed via conductance versus time measurements. Figure 3a, b, and c show an appreciable decrease in electrical conductance of type I devices upon exposure to the proteins hCG, human IgG, and BSA (each at 100 nM), respectively. Top gate $I-V_{gs}$ measurements before and after hCG adsorption (100 nM) also confirm the conductance change (Figure 2).

(16) Shim, M.; Wong Shi Kam, N.; Chen, R. J.; Li, Y. M.; Dai, H. *Nano Lett.* **2002**, *2*, 285.

(17) Kim, W.; Choi, H. C.; Shim, M.; Li, Y. M.; Wang, D. W.; Dai, H. *Nano Lett.* **2002**, *2*, 703.

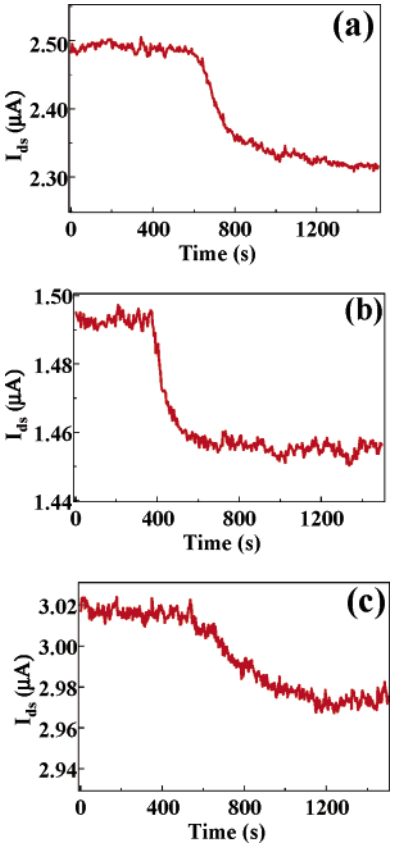

Figure 3. Electrical conductance change of type I devices upon nonspecific binding (NSB) of 100 nM (a) hCG, (b) hIgG, and (c) BSA in aqueous solution. Upon rinsing (data not shown), the conductance does not recover to initial values, indicating that protein adsorbs irreversibly on the devices.

Table 2. Summary of Frequency Changes (in Hz) Measured by QCM Due to Mass Uptake of Various Proteins Adsorbed on Several Types of Surfaces[a]

proteins/ surfaces	Pd	mPEG-SH on Pd	Au	mPEG-SH on Au	pI
BSA	−44.7	−1.7	−9.3	−0.4	4.7
HSA	−52.7	−1.3	−22.4	0.0	4.7
hCG	−99.8	−3.5	−56.0	−3.5	∼5
α-hCG	−147.3	−3.7	−80.2	−7.2	∼7
hIgG	−162.3	−12.9	−140.7	−11.5	∼7
avidin	−130.0	−0.2	−79.1	−3.3	10−11

[a] The table shows that mPEG-SH SAMs on Pd and Au surfaces significantly suppress nonspecific binding of proteins.

The results of the NSB experiments on type I devices agree with previous work on SWNT-based electrical biosensors and confirm that protein adsorption on our micromat devices does modulate conductance. However, characterization and interpretation of the sensing mechanisms have previously focused only on protein adsorption on nanotubes, while ignoring adsorption on the electrodes contacting the nanotubes. Through QCM measurements, the current work finds considerable irreversible adsorption of proteins onto both the Pd and Au surfaces that are used as electrode materials for our sensor devices (Table 2). XPS measurements further confirm substantial protein adsorption on bare Pd and Au surfaces (Table 3 and Figure 4a), as evidenced by the emergence of an N peak observed after protein exposure (nitrogen constitutes a large fraction of protein chemical composition). These results show that, for actual devices, protein NSB occurs to a significant degree not only on carbon nanotubes but also on the metal contacts.

Table 3. X-ray Photoelectron Spectroscopy Data Quantifying Elemental Composition of Various Surfaces before and after Exposure to HCG in Solution[a]

surfaces/ elements	C (%)	N (%)	O (%)	S (%)	Pd (%)
Pd	23.5	0	32.5	0.8	43.1
Pd exposed to protein (hCG)	37.2	8.4	21.3	0.7	32.5
Pd with mPEG-SH SAM	36.6	0.8	21.4	7.9	33.2
Pd with SAM exposed to protein (hCG)	44.1	0.9	19.2	8.7	27.1

[a] The table shows significant NSB of protein on bare Pd surfaces (second row) and negligible adsorption on mPEG-SH coated Pd surfaces (fourth row).

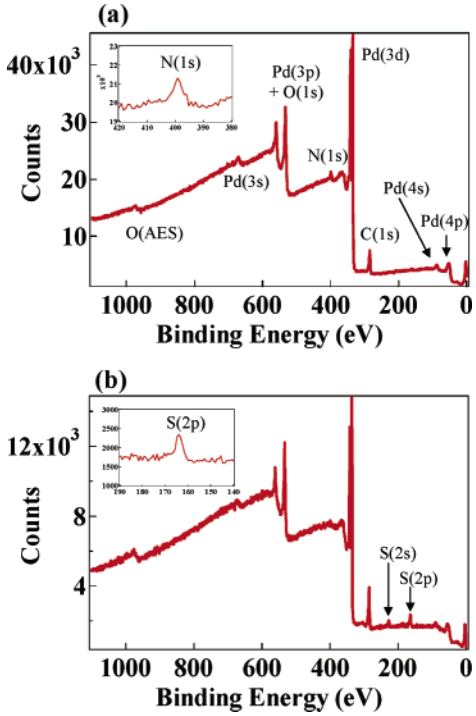

Figure 4. X-ray photoelectron spectroscopy data recorded on (a) a bare Pd surface after immersion in an hCG solution and (b) an mPEG-SH SAM coated Pd surface after the same immersion. A considerable nitrogen peak (∼398 eV, N_{1s}) emerges on bare Pd (inset of a) due to significant protein NSB. There is no indication of protein adsorption on the mPEG-SH coated surfaces while sulfur (∼163 eV, S_{2p}) is observed from the thiol (inset of part b).

Device Type II. To isolate protein adsorption on the metal contacts versus that on nanotubes and to better clarify their respective effects on the conductance of the devices, NSB experiments were conducted in which the Pd (or Pd/Au) metal contacts of devices were selectively modified in such a way as to prevent protein adsorption on the metal but allow it on the nanotubes. This was achieved by covalently binding poly(ethylene glycol) (PEG) to the metal via Pd−S (or Au−S) bond formation with mPEG-SH (10 mM).[18−20] Poly(ethylene glycol) is a biocompatible polymer well-known for its protein repelling properties. Whether covalently or noncovalently immobilized onto substrates such as metals,[21] glass,[22] and even carbon nano-

(18) Nuzzo, R. G.; Allara, D. L. *J. Am. Chem. Soc.* **1983**, *105*, 4481.
(19) Bain, C. D.; Troughton, E. B.; Tao, Y. T.; Evall, J.; Whitesides, G. M.; Nuzzo, R. G. *J. Am. Chem. Soc.* **1989**, *111*, 321.
(20) Love, J. C.; Wolfe, D. B.; Haasch, R.; Chabinyc, M. L.; Paul, K. E.; Whitesides, G. M.; Nuzzo, R. G. *J. Am. Chem. Soc.* **2003**, *125*, 2597.
(21) Ostuni, E.; Chapman, R. G.; Liang, M. N.; Meluleni, G.; Pier, G.; Ingber, D. E.; Whitesides, G. M. *Langmuir* **2001**, *17*, 6336.
(22) Lee, S.-W.; Laibinis, P. E. *Biomaterials* **1998**, *19*, 1669.

tubes,[16] PEG presents an effective barrier against unwanted protein adsorption by forming a highly hydrophilic, but charge-neutral, sterically hindering layer at the surface.[21] By applying mPEG-SH during the microfabrication step before photoresist lift-off (Scheme 1), we obtained type II devices in which the metal contacts were completely passivated with mPEG-SH and were also able to eliminate any potential for nonspecific binding of the thiol onto the nanotubes. This scheme ensures the nanotubes remain bare and completely exposed to solution, exactly as in type I devices. Both QCM and XPS results confirmed that protein adsorption was effectively blocked on Pd and Au after passivation with mPEG-SH (Tables 2 and 3 and Figure 4b).

Previous work has been reported in which the metal contacts of carbon nanotube devices were coated with epoxies and polymers and a lithographically patterned gap opened over the nanotubes,[23] but we believe thiolation presents distinct advantages. Thiols are well-known to form ordered SAMs on Au surfaces as well as on Pd;[20] this self-assembly process, as integrated into the microfabrication, enables metal passivation to the very edges of the electrodes (Scheme 1), a feature impossible to achieve by subsequent lithographic patterning. Uniform monolayer coverage, as can be realized with thiolation, is also key to minimizing the disruption to the electrical and physical properties of the SWNT-device that can occur with thick polymer coatings. Further, these covalent metal−thiol bonds are stable and chemically robust, desorbing only after prolonged exposure to an oxidative atmosphere, high temperatures or by electrochemical reduction.[24] Note that type II devices with mPEG-SH-coated electrodes still exhibit substantial gate dependence (data not shown), similar to type I devices. This suggests that the electronic properties of type II devices have not been significantly altered from those of type I by thiolation of the electrodes and that field effect transistor behavior is preserved.

With type II devices in hand, analogous protein adsorption measurements were carried out, revealing quite different results from those of type I devices. As can be seen from Figures 5a−c, exposure of the metal-passivated devices to the same proteins at the same concentration as before gives no conductance change, even though adsorption does actually occur significantly on the initially bare nanotube surfaces between the SAM-covered electrodes, as evidenced by AFM (Figure 5d). Experiments were also performed (S. Bangsaruntip and H. Dai, unpublished results) in which various benzenethiols were used in place of mPEG-SH in the preparation of type II devices. These alternate devices showed a significant decrease in conductance upon protein exposure, similar to the behavior seen with type I devices. As well as further confirming the vital role the mPEG component plays in blocking protein adsorption, this result underscores the fact that thiolation by itself does not significantly alter the electrical sensitivity of the nanotube devices to protein adsorption.

This discovery introduces a new consideration to the proposal that conductance changes are due to charge injection or field effects caused by proteins adsorbed solely along the lengths of the nanotubes.[9,11] Our results indicate this contribution is not the primary mechanism underlying conductance changes in nanotube devices; instead, protein adsorption on or very near

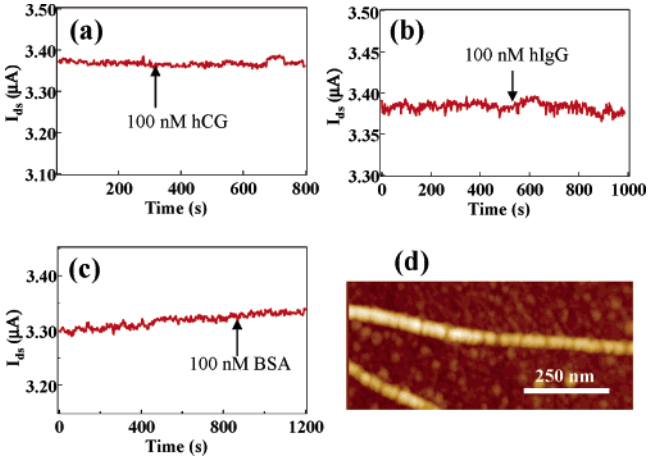

Figure 5. Electrical data recorded during exposure of type II devices (with mPEG-SH SAMs on Pd/Au electrodes) to (a) hCG, (b) hIgG, and (c) BSA in aqueous solution. No obvious electrical response is seen with the addition of 100 nM concentrations of each protein (indicated with arrows). (d) An AFM image of a region between the electrodes in a type II device after exposure to hCG. The image reveals significant protein adsorption on nanotubes, yet no electrical signal is observed since proteins are not adsorbed on the mPEG-SH coated electrodes.

the metal−nanotube contacts appears to be the key to conductance modulation and electrical sensing. Indeed, recent reports indicate that the metal−nanotube interface or contact region is highly susceptible to modulation by adsorbed species.[25,26] The modulation of metal work function, for instance, can alter the Schottky barrier of the metal−nanotube interface, leading to a significant change in the nature of the contacts and consequently a change in the conductance of the devices.[24,27]

Based on these results, we propose that the actual sensing region which is most responsible for the conductance modulation is localized near the edge of the nanotube−metal contact, that is, at or near the point where carbon nanotube and metal meet. Here, the electronic properties of the metal−nanotube contact are altered by protein adsorption, and the change appears to be equivalent to a reduction of the work function of the metal, since the conductance of these p-type devices always exhibits a decrease upon protein adsorption. The Schottky barrier to the valence band of the nanotubes is essentially zero with Pd contacts;[28] therefore, this decrease in conductance is consistent with an increased barrier due to a lowered metal work function.[27] In general, adsorption of various types of species is known to affect the work function of metal surfaces[28] or to induce metal-semiconductor interfacial potentials or dipolar changes (if the work function concept is not invoked). It is noted that changes in the concentration of buffering salts in the solution can induce electrical conductance changes in type I devices. Adsorption of other species, such as surfactants, likewise causes the conductance to change. A detailed explanation for these effects would require further study; however, we speculate that the metal−nanotube contacts play a role in the conductance modulation here as well.

(23) Someya, T.; Kim, P.; Nuckolls, C. *Appl. Phys. Lett.* **2003**, *82*, 2338.
(24) Sumi, T.; Wano, H.; Uosaki, K. *J. Electroanal. Chem.* **2003**, *550*, 321.
(25) Cui, X. D.; Freitag, M.; Martel, R.; Brus, L.; Avouris, P. *Nano Lett.* **2003**, *3*, 783.
(26) (a) Appenzeller, J.; Knoch, J.; Derycke, V.; Martel, R.; Wind, S.; Avouris, P. *Phys. Rev. Lett.* **2002**, *89*, 126801. (b) Heinze, S.; Tersoff, J.; Martel, R.; Derycke, V.; Appenzeller, J.; Avouris, P. *Phys. Rev. Lett.* **2002**, *89*, 106801.
(27) Javey, A.; Guo, J.; Wang, Q.; Lundstrom, M.; Dai, H. *Nature* **2003**, *424*, 6949.
(28) (a) Kizhakevariam, N.; Jiang, X.; Weaver, M. *J. Chem. Phys.* **1994**, *100*, 6750. (b) Villegas, I.; Weaver, M. J. *J. Chem. Phys.* **1995**, *103*, 2295. (c) Villegas, I.; Weaver, M. J. *J. Am. Chem. Soc.* **1996**, *118*, 458.

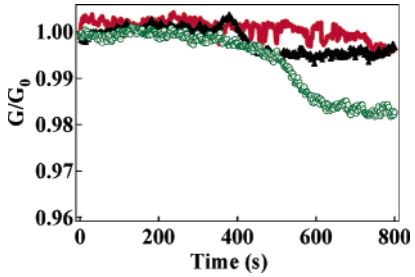

Figure 6. Electrical data recorded upon exposure to avidin of a type I device (circle), an mPEG-SH coated Pd/Au electrode device (type II, triangle), and a mPEG-SH/Tween 20-coated device (device type III, solid).

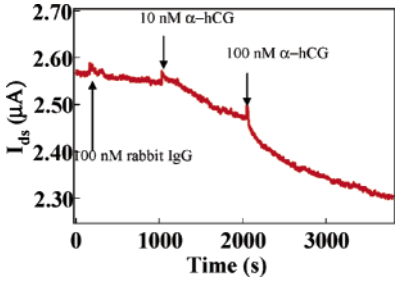

Figure 7. Electrical data shows selective sensing of α-hCG against rabbit IgG with a type I device preadsorbed with hCG.

The current device design, however, does not allow for a quantitative measurement of these changes occurring at the contacts due to the ensemble nature of the nanotubes used in the devices; that is, the electronic characteristics correspond to a mixture of different types of nanotubes. We are therefore currently developing an individual semiconducting nanotube device for biosensors, the transistor characteristics of which will enable a meaningful extraction of various parameters, including those for the contacts before and after protein adsorption.

Device Type III. A highly positively charged protein, avidin (pI 10−11), is found to be still capable of inducing a drop in conductance not only with the nonpassivated type I devices (Figure 6, circle) but also with type II devices with metal electrodes passivated by mPEG-SH (Figure 6, triangle). In this exceptional case among all of the proteins tested, additional NSB resistance can be imparted to the nanotubes in the form of a Tween 20 coating (device type III).[9] After such treatment, exposure to avidin no longer affects the conductance of the devices (Figure 6, solid line), owing to effective repulsion of avidin from the nanotube surface. Apparently, the contribution of gating the exposed lengths of nanotubes via charge transfer through adsorption on the nanotube sidewalls, though usually negligible for other proteins, as shown previously, becomes discernible with highly positively charged species such as avidin. It should be noted that most proteins of interest, including all others used in this work, lie within a pI range of 5−7. At physiological pH, these proteins are essentially neutral or slightly charged and, therefore, do not require additional NSB resistance beyond electrode passivation.

Selective Second Layer Detection. Adsorption of proteins onto the surface of type I micromat devices by simple NSB can be utilized for the selective detection of a second protein which shows binding affinity for the first. Such biospecific pairs have been used to enable a wide variety of devices toward selective biomolecular detection, biotin/avidin, antigen/antibody, ss-DNA hybridization, etc. As a test for second layer selective sensing capability with the new micromat design, the hCG/α-hCG antigen/antibody binding pair was chosen as an initial study. hCG, human chorionic gonadotropin, is a hormone that is produced during pregnancy and serves as the basis for many clinical pregnancy tests; α-hCG is the corresponding monoclonal antibody raised specifically to bind with high selectivity to hCG. hCG was first allowed to adsorb nonspecifically onto a type I micromat device, affording the expected decrease in conductance as seen in Figure 3a. The device was thoroughly rinsed and then exposed to rabbit IgG (100 nM) as a control for selectivity (Figure 7, first arrow). Lack of a significant signal after this addition indicated successful blocking of a structurally similar but nonspecific IgG. 10 nM α-hCG was then added, whereupon a signal change was observed, indicating a successful binding of α-hCG to the device preadsorbed with hCG (Figure 7, second arrow). α-hCG at the 100 nM concentration level yielded an additional, relatively proportionate, response (Figure 7, third arrow).

Conclusion

Hybrid structures combining the unique electronic properties of nanoscale materials such as carbon nanotubes with the exceptional molecular recognition capabilities inherent in biological molecules such as antibodies and DNA provide interesting opportunities for future nanobiotechnologies. Miniaturized nanotube biosensors, such as presented in this report, may facilitate advances in understanding complex biological processes and usher in a new paradigm in true bioelectronic materials. As a first step, we have demonstrated miniaturized arrayable SWNT-based biosensors. These sensor arrays have the potential of being functionalized and addressed in multiplex fashion via innovative approaches. This new geometry, for the first time, allows a systematic investigation into the mechanistic aspects of solution-phase biosensing with nanotube FETs. Our data leads to the conclusion that much of the conductance changes due to protein binding on nanotube FET devices originate from the metal−tube contact region. Schottky barrier modulation at the metal−nanotube contacts of such devices due to biomolecular adsorption likely dominates the conductance change. Proteins with a pI of 5−7 show appreciable conductance change upon adsorption on bare devices but none on those in which the metal contacts have been passivated with mPEG-SH. Anomalous behavior with the protein avidin (pI 10−11) reveals that the normally negligible contribution from adsorption on the exposed lengths of the nanotubes is magnified to a significant and detectable degree when the species is highly charged.

Building on these results, we are currently developing next generation nanotube based biosensors for additional mechanistic studies and multiplex functionalized electronic sensor arrays. By elucidating the complex relationship between carbon nanotubes and metal contacts and their respective interaction with proteins, and further advancing chemical functionalization approaches, future nanotube FET designs can be further optimized for increased sensitivity and selectivity for aqueous-phase biosensing.

Acknowledgment. This work was supported by DARPA/MTO, the Stanford Interdisciplinary Translational Research Program, the Stanford CPIMA, a Sloan Research Fellowship, Packard Fellowship, and a Dreyfus Teacher-Scholar Award.

JA038702M